

Indium distribution in InGaAs quantum wires observed with the scanning tunneling microscope

M. Pfister,^{a)} M. B. Johnson,^{b)} S. F. Alvarado, and H. W. M. Salemink
IBM Research Division, Zurich Research Laboratory, 8803 Rüschlikon, Switzerland

U. Marti, D. Martin, F. Morier-Genoud, and F. K. Reinhart
Institut de Micro- et Optoélectronique, Ecole Polytechnique Fédérale, 1015 Lausanne, Switzerland

(Received 10 April 1995; accepted for publication 28 June 1995)

The incorporation of In in the growth of crescent-shaped $\text{In}_{0.12}\text{Ga}_{0.88}\text{As}$ quantum wires embedded in $(\text{AlAs})_4(\text{GaAs})_8$ superlattice barriers is studied in atomic detail using cross-sectional scanning tunneling microscopy. It is found that the In distribution in both the surface and the first subsurface layer can be atomically resolved in the empty- and filled-state images, respectively. Strong In segregation is seen at the InGaAs/GaAs interfaces, but neither an expected enhancement of the In concentration at the center of the quantum wire compared to the planar quantum well nor In clustering beyond the statistical expectation is observed. © 1995 American Institute of Physics.

Epitaxial growth on prepatterned substrates can be used to fabricate crescent-shaped quantum wires (QWRs).^{1,2} When growing a ternary material such as InGaAs, variations of the ternary alloy composition may occur due to different lateral migration lengths and incorporation rates of the group-III species. Similarly, surface segregation of In in the growth direction occurs³ and leads to rough InGaAs/GaAs interfaces. The atomically precise observation and quantification of these effects is very difficult using conventional methods, because they average in at least one dimension over many atomic layers. On the other hand, cross-sectional scanning tunneling microscopy (XSTM) has chemical sensitivity on an atomic scale within the group-III sublattice of III-V heterostructures.⁴ In fact, Zheng *et al.*⁵ have recently used it to study a planar InGaAs/GaAs heterostructure.

In this letter, we report on the characterization by XSTM of InGaAs QWRs grown by molecular beam epitaxy (MBE). It is shown that In atoms can be atomically resolved not only in the cross-sectional surface layer, but also in the *first subsurface layer*. The measured In distribution clearly reveals In segregation in the growth direction. No preferential incorporation of In at the center of the crescent-shaped QWR is seen, and the substitutional In is found to be randomly distributed on the group-III sublattice, i.e., no short-range In clustering beyond the statistical expectation is observed.

The sample discussed in this letter consists of a series of InGaAs QWRs and planar control quantum wells (QWs) grown by MBE at 540 °C on a V-groove-patterned GaAs *n*-type substrate. The V-grooves having side wall facets close to $\{311\}\text{B}$ planes and a periodicity of 250 nm are fabricated using holographic lithography and wet etching.² The undoped InGaAs layers are embedded in 16 monolayers (ML) of GaAs and 8.5 periods of a moderately Si *n*-doped $(\text{AlAs})_4(\text{GaAs})_8$ superlattice (SL) barrier. The QWR and QW layers nominally consist of 18 ML of $\text{In}_x\text{Ga}_{1-x}\text{As}$, where $x = 12\%$. Growth was interrupted for 20 s after every 3 ML

to promote the formation of the crescent-shaped wire and in an attempt to enhance the In concentration within the wire. STM measurements were performed in ultrahigh vacuum (1×10^{-11} mbar) using electrochemically etched W tips. The sample is cleaved *in situ* to expose an atomically flat, electronically unpinned (110) surface. Images with both positive and negative sample bias (sensitive to empty and filled surface states, respectively⁶) were acquired in a constant current mode.

Figures 1(a) and 1(b) show empty-state (group-III-related) STM images of the cross section of an InGaAs QW and QWR, respectively, acquired with a positive sample bias of $V_s = +1.9$ V. Linecuts along the $[001]$ -oriented atomic columns indicated are shown in Fig. 1(c). These lines illustrate that the observed contrast consists of a slowly varying contribution from the “bulk” (subsurface material) as well as an atomically resolved part from the empty surface states. The former is related to the electronic band structure, whereas the latter yields chemical sensitivity, as is discussed in detail below. Figure 2(a) is an enlarged empty-state view of the center of the QWR with the slowly varying background contrast removed, and Fig. 2(b) is the corresponding filled-state image (group-V-related) of *the exact same area* acquired with $V_s = -2.3$ V. Although the two images were not taken simultaneously, it is possible to align them by adjusting the position of the imaged defects in the surface.

The appearance of the $(\text{AlAs})_4(\text{GaAs})_8$ SL in the empty-state image in Fig. 1 is different from that observed in filled-state images, e.g. at the top of Fig. 2(b). Whereas the presence of 4 ML of AlAs leads to two quite sharply defined darker rows in the filled-state image,⁷ the layer contrast is much less distinct in the empty-state images. We attribute this behavior to the fact that empty-state imaging involves the tunneling of electrons into conduction-band states having a much lower effective mass than the hole states in the valence band involved in filled-state imaging. These conduction-band states are therefore more delocalized in such a short-period SL and result in less distinct contrast.

The center of the QWR in Fig. 1 appears brighter than the planar QW. Two mechanisms may contribute to this dif-

^{a)}Also at: IMO-DP, EPFL, 1015 Lausanne, Switzerland. Electronic mail: pfm@zurich.ibm.com

^{b)}Present address: Dept. of Physics and Astronomy, University of Oklahoma, Norman, OK 73072.

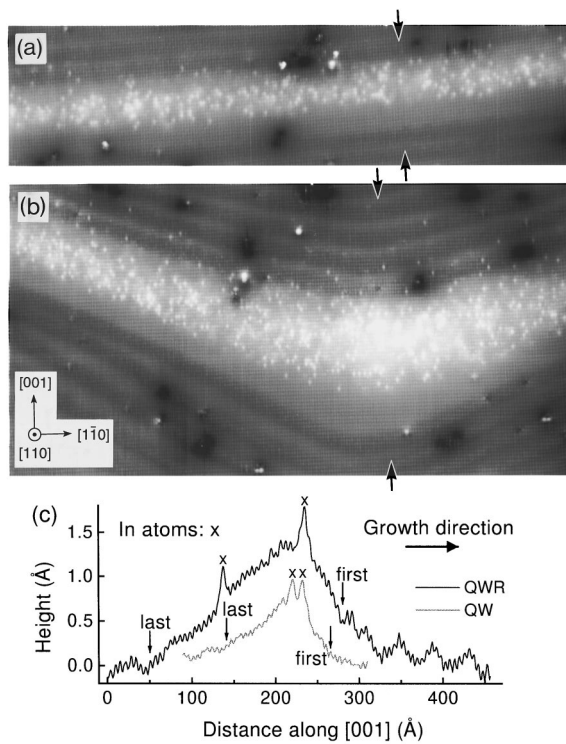


FIG. 1. STM empty-state cross-sectional images of (a) an $\text{In}_{0.12}\text{Ga}_{0.88}\text{As}$ QW embedded in $(\text{AlAs})_4(\text{GaAs})_8$ SL barriers (scan size $800 \times 220 \text{ \AA}^2$) and (b) a similarly embedded QWR grown on $\{311\}$ B-type side walls (scan size $800 \times 450 \text{ \AA}^2$). Tunneling conditions: sample bias +1.9 V and tunneling current 40 pA. The gray-scale range is 0.6 \AA in both images. Individual In atoms appear as atomically sharp white dots. (c) Linecuts across the QWR and the QW along the $[001]$ -columns indicated in (a) and (b). “First” and “last” mark the start and end of the SL barriers.

ference: (i) the ground state of the QWR is lower in energy and more states are available for tunneling, and (ii) there is more strain relaxation at the free surface in the QWR case.

Examination of the images on the atomic scale yields chemical information. An empty-state image [see especially Fig. 2(a)] directly probes the energy and spatial extent of dangling bonds associated with group-III sites. In the GaAs regions the corrugation is regular, whereas in the InGaAs regions atomically localized white features, corresponding to In atoms in the surface layer, are observed. The In atoms in the surface appear white for two reasons. First, the In atom is larger than the Ga atom, so the dangling bond extends further out of the surface. Second, the energy associated with the In dangling bond is lower than that of the corresponding Ga bond (InAs has a lower band gap than GaAs). The larger energy difference between tip and In bond causes In to appear brighter in a constant current image. Importantly, the percentage of white sublattice sites is close to the nominal In concentration, which supports this interpretation.

The filled-state image, Fig. 2(b), directly probes the energy and spatial extent of the As dangling bonds of the region imaged in Fig. 2(a). Surprisingly, this image also shows atomically localized white features similar to the In features of the empty-state image.⁸ Like in the empty-state image, the percentage of white sublattice sites is close to the nominal In concentration. The positions of the strong filled-state white

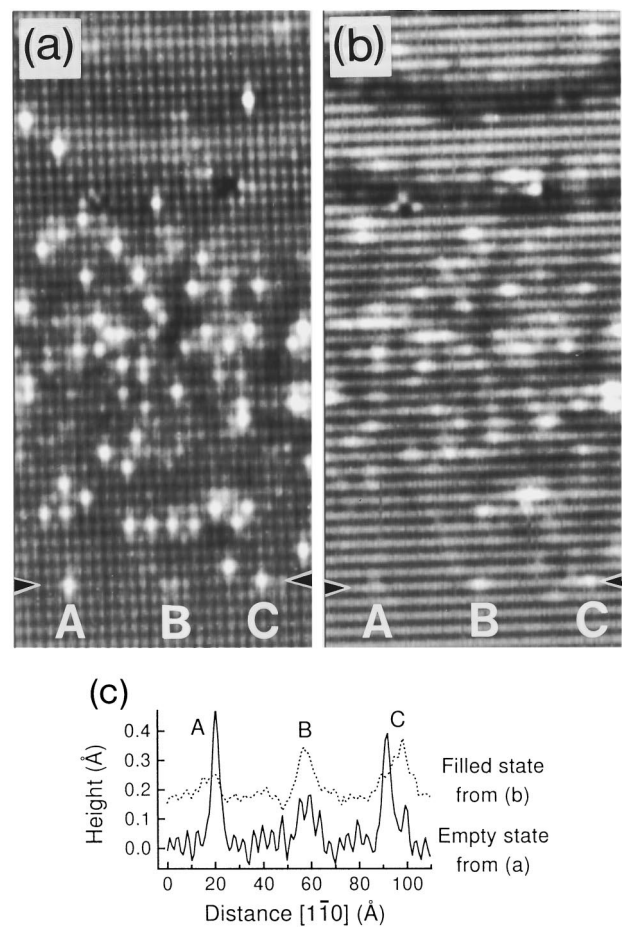


FIG. 2. (a) Empty- and (b) filled-state images of exactly the same $112 \times 250 \text{ \AA}^2$ region of the QWR. The white features represent In atoms in the surface and subsurface (110) layers. The In distributions are random and uncorrelated. (c) Linecuts through the same atomic row (indicated in the images) showing a surface In, a subsurface In, and adjacent surface and subsurface In atoms, labeled A, B and C, respectively.

features *do not correlate* with the empty-state In features, but faint filled-state features do correlate with the empty-state In positions as shown, for example, at “A” in Fig. 2(c), which displays linecuts along the same $[1\bar{1}0]$ -oriented zigzag line. Inversely, faint empty-state double-site features also correlate with the filled-state white features as shown at “B”. This evidence suggests that the filled-state white features must themselves be independent In atoms, not in the surface, but in the first subsurface layer, where In is in the back-bond position below the imaged As sites. Here, the white atomic features may be attributed to the As atom being pushed out of the surface by the large In and/or a higher energy As dangling bond resulting from In in the back-bond position. The weak influence of a surface In on its two neighboring As atoms (label “A”) suggests that the geometric effect is the predominant contrast mechanism. Further strong evidence of this is given by spectroscopic filled-state images (not shown here), which exhibit a voltage-independent appearance of the subsurface In over the range $V_s = -1.7$ to -3.0 V, contrary to the electronic contrast of the SL, which disappears rapidly at higher voltages.⁹ In summary, the white features in the

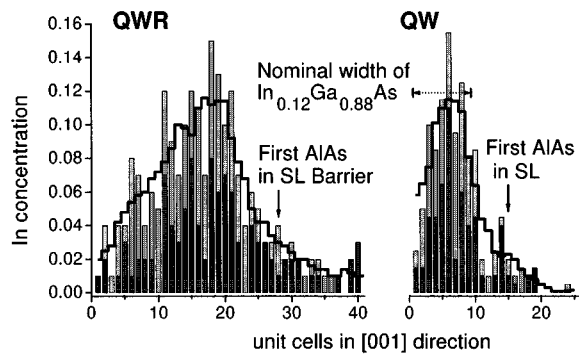


FIG. 3. Indium concentration across of the QWR and QW. Light and dark gray shading indicates the ratio of In atoms counted in the surface (empty-state data) and the first subsurface layer (filled-state data), respectively. The bold line is a running average over five rows. One unit cell in [001] direction equals 2 ML.

filled-state image represent In atoms in the first subsurface layer, and those in the empty-state image represent In in the top surface. For example, “C” in Fig. 2(c) corresponds to an In atom in the surface layer about one and one-half lattice sites to the left of an In atom in the first subsurface layer.

The above results enable us to count In atoms in the group-III sublattice in the *first two (110)-oriented layers*, therefore producing better statistics. This is especially important in the case of the QWR for which the cross-sectional area observed is relatively small. Figure 3 displays histograms of the In concentration across the center of the QWR and across the QW. The concentration within one bar is obtained by counting In atoms over a width of 20.0 nm (50 lattice sites) in the case of the QWR — a width over which the QWR does not “bend” much — and over 40.0 nm (100 lattice sites) in the case of the QW. A running average over five rows is also plotted. We find that for both the planar reference QW and the (311)-V-groove QWR, there is a maximum In concentration of $11.5 \pm 1.4\%$. The statistical error is calculated for the averaged data, and systematic counting errors are assumed to be the same for the QW and the QWR.

We have also indicated the width of the nominally 18-ML-thick $\text{In}_{0.12}\text{Ga}_{0.88}\text{As}$ QW. Buildup of the nominal In concentration occurs over about 6 ML. This differs from the QWR, where buildup is slower. This is only partially due to the averaging over a width of 20 nm. It may indicate that during this growth with interruptions of 20 s every 3 ML, the Ga atoms have enough time to migrate and be incorporated at this energetically favorable position. For the In atoms the tendency to segregate on the growth surface seems to predominate. On the top interface, strong In segregation occurs that is apparently not significantly inhibited by the growth of the $(\text{AlAs})_4$ layers in the SL above.

Zheng *et al.*⁵ reported that the In in a $\text{GaAs}/\text{In}_{0.2}\text{Ga}_{0.8}\text{As}/\text{GaAs}$ sample grown by MBE at the same growth temperature as here, but without the 20 s growth interruptions, exhibited strong preferential clustering in the [001] growth direction. We found that in our case In is not clustered beyond statistical expectations. Figure 4 shows histograms of In cluster sizes in an area of the QW having quite a uniform In concentration of 10% and in an area of the QWR

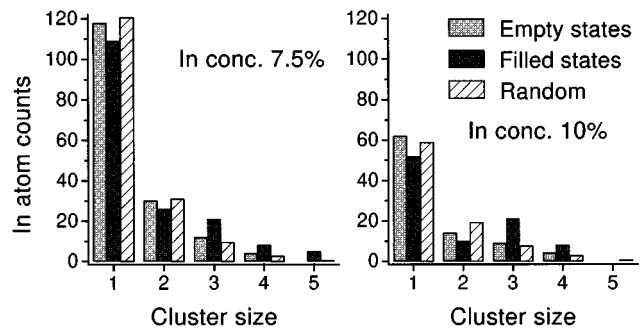


FIG. 4. Cluster size (Ref. 10) distribution in a QWR area with 7.5% In (left) and in a QW area with 10% In (right).

where the In concentration is 7.5%. The bars labeled “Random” are the total number of In counts multiplied by the probability of having a certain cluster size.¹⁰ The measured cluster size distribution closely follows this model, which assumes random distribution of the substitutional In in the group-III sublattice. Only in the filled-state measurement and for the horizontal $[1\bar{1}0]$ direction do we find larger clusters. We attribute this to the missing atomic resolution in this direction in the filled-state image, which sometimes makes it difficult to distinguish between two In atoms and a cluster of three In atoms, for example.

In conclusion we have shown that in the case of the ternary InGaAs material, STM empty- and filled-state images show the In distribution in the (110) surface and the first subsurface layer, respectively. To within statistical error, we observe no preferential In incorporation in the crescent-shaped QWR at the bottom of the V-groove compared to a planar QW reference. Strong In segregation is seen into the SL barriers. The cluster size distribution shows that In is randomly distributed on the group-III sublattice.

We acknowledge P. Silva and Y. Magnenat for assistance in sample preparation, as well as P. Blöchl and A. Baldereschi for valuable discussions. This work was supported by the Swiss Priority Program in Optics and the Swiss National Science Foundation, contract No. 21/34317.92.

¹E. Kapon, *Optoelectronics* **8**, 429 (1993).

²U. Marti, M. Proctor, D. Martin, F. Morier-Genoud, B. Senior, and F. K. Reinhart, *Microelectronic Engineering* **13**, 391 (1991).

³J. Massies, F. Turco, A. Salates, and J. P. Contour, *J. Cryst. Growth* **80**, 307 (1987).

⁴H. W. M. Salemink and O. Albrektsen, *Phys. Rev. B* **47**, 16044 (1993).

⁵J. F. Zheng, J. D. Walker, M. B. Salmeron, and E. R. Weber, *Phys. Rev. Lett.* **72**, 2414 (1994).

⁶R. M. Feenstra, J. A. Stroscio, J. Tersoff, and A. P. Fein, *Phys. Rev. Lett.* **58**, 1192 (1987).

⁷M. Pfister, M. B. Johnson, S. F. Alvarado, H. W. M. Salemink, U. Marti, D. Martin, F. Morier-Genoud, and F. K. Reinhart, *Appl. Phys. Lett.* **65**, 1168 (1994).

⁸In the filled-state image in Fig. 2(b), the white features appear slightly elongated due to the lack of atomic resolution in the $[1\bar{1}0]$ direction. In other filled-state images they clearly occupy only a single lattice site.

⁹M. Pfister, M. B. Johnson, S. F. Alvarado, H. W. M. Salemink, U. Marti, D. Martin, F. Morier-Genoud, and F. K. Reinhart (unpublished).

¹⁰Cluster size 1 is an In atom that has no In neighbor one unit cell to the left, to the right, above or below. The probability of such a configuration in $\text{In}_x\text{Ga}_{1-x}\text{As}$ is $(1-x)^4$. Diagonal configurations are not taken into account.